Effect of the Surface Diffusion and Evaporation of Impurities on Step Bunching Induced by Impurities

Effect of the Surface Diffusion and Evaporation of Impurities on Step Bunching Induced by Impurities

Masahide Sato

Information Media Center, Kanazawa University, Kanazawa 920-1192, Japan

(Dated: October 10, 2019)

Abstract

We consider a vicinal face, where atoms and impurities impinge and evaporate to a vapor phase, to study how the surface diffusion and evaporation of impurities affect step bunching induced by impurities. When the lifetime of impurities on the vicinal face τ_{imp} is long and the surface diffusion of impurities is neglected, the step bunches induced by impurities are tight. When τ_{imp} decreases, the size of the step bunches, which means the number of steps in the bunches, decreases but the separation of single steps from bunches does not occur. When we take into account fast surface diffusion of impurities, the separation and collision between single steps and step bunches occur repeatedly.

PACS numbers: 61.50.Ah, 81.15.Aa ,81.10.Aj

I. INTRODUCTION

Step bunching is well-known to be induced by impurities. Many groups have studied the theory underlying step bunching [1–12]. By assuming that the velocity of a single step decreases with increasing the impurity density on a surface, Frank [2] was able to explain why step bunching is caused by impurities. In that model, the impurity density increases until advancing steps refresh the surface. The time evolution of the number of steps in bunches during the step bunching was studied using a one-dimensional model [3, 4], in which the dependence of the step velocity on the terrace width was assumed empirically. From Monte Carlo simulations, Weeks and co-workers [5, 8, 9] were able to study two-dimensional step motion and showed that mesh-like step bunch patterns are formed by step bunching. In their model, the effect of impurities is taken into account as a reduction in the probability of step advancing. Sluetel and co-workers [11] also studied step bunching induced by impurities using another type of model. They showed that macrosteps formed by impurities can advance under high impurity conditions in which elementary steps cannot advance.

Those models used in the previous studies [1–12] are simple and useful, but the surface diffusion field formed by adatoms is neglected and motions of impurities are not taken into account concretely. Therefore, we developed a model in which those processes were adopted and studied the step bunching induced by impurities performing Monte Carlo simulations [13, 14]. We suppose that both atoms and impurities impinge from a vapor phase to a vicinal face with impingement rates F and F_{imp}, respectively. We assume that impurities are contained in materials with a constant ratio. Under that assumption, the ratio of F_{imp} to F should be kept constant if F changes. Therefore, we kept F_{imp}/F constant in our simulations. In our previous studies [13, 14], we neglected the surface diffusion of impurities and studied how step bunching induced by impurities depends on F. When neither impurities nor adatoms evaporate from a vicinal face [13], step bunching is caused by small F. The impurity density on the surface σ_{imp} increases when step bunches are formed. We also studied step bunching in two other systems: one is the system in which only impurities evaporate, and the other is the system in which both atoms and impurities evaporate [14]. When only impurities evaporate, the step bunching is induced by small F, which is the same as that in the system where neither impurities nor adatoms evaporate [13].

When large bunches are formed, σ_{imp} increases but the density of impurities incorporated in solid ρ_{imp} decreases. When both impurities and adatoms evaporate, σ_{imp} and ρ_{imp} increase because of step bunching.

Separation of single steps from bunches did not occur in our previous studies [13, 14]. We wondered why the separation of steps, which is observed during step bunching in other systems [15–17], does not occur in our previous simulations for impurity-induced step bunching [13, 14]. We suggest that the separation of single steps may occur repeatedly when we change the lifetime of impurities τ_{imp} or take into account the surface diffusion of impurities. Therefore, in our study, we performed Monte Carlo simulations and studied the effects of both the surface diffusion of impurities and the lifetime of impurities on the separation of single steps. In Sec. II, we introduce our model, in which we add the surface diffusion of impurities to our previous model [14]. In Sec. III, we show the results of our simulations. In Ref. 18, the difference in the Ehrich-Schwoebel barrier [19, 20] between dimers and monomers causes step bunching during growth. In that study, the distribution of terrace width changes with the variation in the impingement rate of monomers, the coefficient of diffusion of monomers, and the average terrace width on a vicinal face. Although the cause of step bunching is different in our model, we show that the distribution of terrace widths changes by controlling parameters even in our system. In Sec. III A, we show the dependence of the form of step bunches on τ_{imp}. In Sec. III B, we show the relationship between the separation of steps and the frequency of the surface diffusion of impurities. In Sec. IV, we summarize our results.

II. MODEL

In general, kinetic Monte Carlo simulations are based on implementing a set of events with given rates. We just have to perform the events according to the rates. However, we adopted another approach used in previous studies [21–24]. This approach is not effective but it is easy to consider the correspondence with the Burton–Cabrera–Frank (BCF) model [2]. We discretize the diffusion equation of adatoms and consider particles hopping on a lattice, which correspond to adatoms. Hopping of particles, and solidification and melting at steps occur probabilistically. Because solid atoms and adatoms are distinguished in the model, we can define the step stiffness $\tilde{\beta}$ and the equilibrium adatom density c_{eq} independently.

3

We modify the models adopted in our previous studies [13, 14] and conduct Monte Carlo simulations.

We consider a square lattice, in which the lattice constant is unity. The system lengths in the x and y-directions are denoted by L_x and L_y, respectively. We use a periodic boundary condition in the x-direction and a helical boundary condition in the y-direction. Initially, straight N steps are set parallel to the x-axis. The steps advance to the y-direction during growth. For simplicity, we forbid two-dimensional nucleation on terraces.
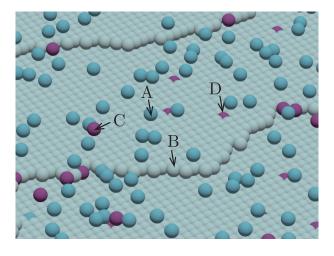

FIG. 1. (color online) Schematic of our model. Particles (A), (B), (C), and (D) are an adatom, a solid atom forming step, an impurity on a surface, and an impurity incorporated into a solid, respectively.

In our simulation, we choose adatoms, impurities on surface, or solid atoms having empty neighboring sites in the horizontal direction, and try surface diffusion of both adatoms and impurities, solidification of adatoms, or melting of solid atoms. When we choose either an adatom such as particle (A) in Fig. 1 or an impurity on the surface such as particle (C) in Fig. 1, we first try the evaporation of the chosen particle. If it does not evaporate, we next try its surface diffusion. As a surface diffusion trial of an adatom, we try to move an adatom to one of its four neighboring sites, where the moving probability is 1/4 for each site. When the selected site is already occupied by an impurity or an adatom, we do not move the selected adatom and make it stay at the same site. Because we set the coefficient of diffusion for adatoms D_s to unity, the time increase in a diffusion trial of an adatom is given by $1/4N_s$, where N_s is the number of adatoms. We assume that the coefficient of the surface diffusion of impurities D_{imp} is smaller than D_s. The rule for the surface diffusion

4

of impurities is the same as that of adatoms except that we determine whether we try the surface diffusion of impurities with a probability $D_{\mathrm{imp}}/(4D_{\mathrm{s}})$. Because the steps are permeable in our model [25], both adatoms and impurities can diffuse on the surface over the steps.

We solidify adatoms when they attach to a step after a diffusion trial. The solidification probability for adatoms p_{s} is given by

$$p_{\mathrm{s}} = \left[1 + \exp\left(\frac{\Delta E - \phi}{k_{\mathrm{B}}T}\right)\right]^{-1}, \tag{1}$$

where ΔE represents the change in the step energy, ϕ the change in the chemical potential by solidification per an adatom, k_{B} the Boltzmann constant, and T temperature. When an adatom attaches to n_{n} solid atoms in the horizontal direction, ΔE is given by $2\epsilon(2 - n_{\mathrm{n}})$, where ϵ is the bonding energy per one bond. For simplicity, we forbid the formation of multi-height steps.

We do not solidify impurities but regard that impurities as incorporated into the solid phase when all their neighboring sites are occupied by solid atoms and impurities such as particle (D) in Fig. 1. The impurities incorporated into the solid phase cannot diffuse on a surface nor evaporate unless one or more of the neighboring sites get empty. We assume that the surface diffusion of both adatoms and impurities on the impurities incorporated into the solid phase is possible.

The lifetimes of adatoms and impurities on a vicinal face are given by τ and τ_{imp}, respectively. They are related to the evaporation probability of adatoms p_{eva} and that of impurities $p_{\mathrm{eva}}^{\mathrm{imp}}$ as $p_{\mathrm{eva}} = 1/4\tau$ and $p_{\mathrm{eva}}^{\mathrm{imp}} = 1/4\tau_{\mathrm{imp}}$. After some evaporation and diffusion trials, impurities and atoms impinge on the sites, which are not occupied by other particles, at random with the impingement rates F_{imp} and F, respectively. When impurities are contained in raw materials, the ratio of F_{imp} to F is probably kept constant even if F changes. Therefore, we performed simulations keeping F_{imp}/F constant

We also try melting of solid atoms, for example particle (B) in Fig. 1, which is a solid atom having an empty neighboring site at least and no adatom on it. When a melting trial succeeds, the melted atom stays on the same site as an adatom. The melting probability p_{m} is given by

$$p_{\mathrm{m}} = \left[1 + \exp\left(\frac{\Delta E + \phi}{k_{\mathrm{B}}T}\right)\right]^{-1}. \tag{2}$$

5

The frequencies of solidification and melting trials are the same at kink sites, where $\Delta E = 0$ in equilibrium. Because the equilibrium adatom density c_{eq} satisfies $c_{eq} p_s = (1 - c_{eq}) p_m$ at the kink sites, c_{eq} is given by [24]

$$c_{eq} = \left[1 + \exp \left(\frac{\phi}{k_B T} \right) \right]^{-1}. \tag{3}$$

For small step fluctuations, the step stiffness $\tilde{\beta}$, which represents the increase in the step free energy by step fluctuation, can be estimated in our model. When we assume that the step position y is a single function of x because of a small step fluctuation, the difference in the step position between neighboring sites $n = (y(x_{i+1}) - y(x_i))/a$ is related to the step stiffness as [24]

$$\tilde{\beta} = \frac{k_B T}{a \langle n^2 \rangle} = \frac{2 k_B T}{a} \sinh^2 \frac{\epsilon}{2 k_B T}, \tag{4}$$

where $\langle n^2 \rangle$ is the ensemble average of n^2. Because $\langle n^2 \rangle$ is as large as the average kink density for small step fluctuations, small $\tilde{\beta}$ means the formation of many kinks.

III. RESULTS OF SIMULATIONS

We set the system size $L_x \times L_y$ to 512×512 and the number of steps N to 16 in our simulations. Initially, the steps are straight and equidistant. The initial number of adatoms is roughly equal to that in equilibrium and impurities are not present on the vicinal face. We set $\epsilon/k_B T = 2.0$ and $\phi/k_B T = 3.0$, which are the same as those used in our previous study [14]. Because the capillary length, which is given by $a^2 \tilde{\beta}/(k_B T)$, is estimated to be 2.76, there are many kinks on the steps. The adatom density under an equilibrium condition is low in the simulation system because c_{eq} is set to 4.7×10^{-2}. Other parameters, F, F_{imp}/F, and τ are set to 1.4×10^{-3}, 4×10^{-3}, and 512, respectively.

A. Dependence of step bunching on the lifetime of impurities

In our previous study [14] with large lifetimes of impurities, stable step bunches are formed and the separation of single steps from bunches, which occurs in other systems [15–17], is not observed. We think that the separation of steps may repeatedly occur when τ_{imp} is small. Hence, we neglect the surface diffusion of impurities for simplicity and study how behaviors of step bunches change by decreasing τ_{imp}.
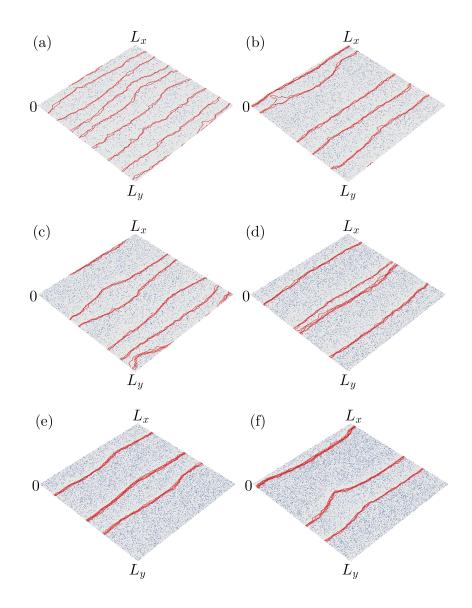
FIG. 2. (color online) Snapshots of step bunches with (a) $\tau_{\mathrm{imp}} = 3 \times 10^4$ at $t = 3.7 \times 10^6$, (b) $\tau_{\mathrm{imp}} = 4 \times 10^4$ at $t = 3.5 \times 10^6$, (c) $\tau_{\mathrm{imp}} = 5 \times 10^4$ at $t = 3.4 \times 10^6$, (d) $\tau_{\mathrm{imp}} = 6 \times 10^4$ at $t = 3.3 \times 10^6$, (e) $\tau_{\mathrm{imp}} = 7 \times 10^4$ at $t = 3.1 \times 10^6$, and (f) $\tau_{\mathrm{imp}} = 8 \times 10^4$ at $t = 3.1 \times 10^6$, where we set $D_{\mathrm{imp}}/D_{\mathrm{s}}$ to 0. The blue dots on the surface represent impurities.

Figure 2 shows snapshots of surfaces in late stages of step bunching for various τ_{imp}, where large bunches are formed and no single steps are seen on large terraces. The bunch size N_{B}, which means the number of steps in a bunch, decreases with decreasing τ_{imp}. As step bunches are straight in each case, we average the step positions in the x-direction and see the time evolution of the average step positions.

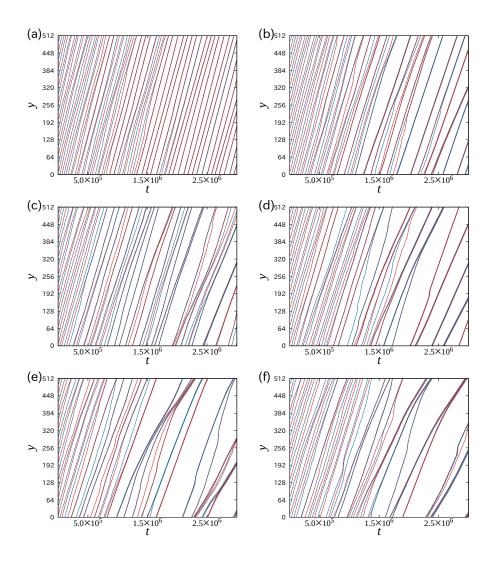Figures 3(a)–(f) show the time evolution of average step positions for the samples used

FIG. 3. (color online) Time evolution of step positions averaged in the x-direction: (a)–(f) for the sample used in Figs. 2(a)–(f), respectively. τ_{imp} is (a) 3×10^4, (b) 4×10^4, (c) 5×10^4, (d) 6×10^4, (e) 7×10^4, and (f) 8×10^4.

in Figs. 2(a)–(f), respectively. The initial equispaced steps are unstable against step fluctuations and small bunches form in the early stages. The bunch size N_{B} increases with the collision of small bunches. Single steps temporarily appear because of the collisions of bunches in the early stages, but the single steps are rarely seen in the late stage. Because we might see rare cases in Figs. 2 and 3, we try ten individual runs for each τ_{imp} and study how the number of isolated steps N_{iso} decreases and N_{B} increases with time.

Figure 4 shows the distributions of terrace widths that are smaller than 16 for $\tau_{\text{imp}} = 3 \times 10^4$ and 1×10^5. The number of small terraces increases with increasing τ_{imp} As N_{B} seems to increase with increasing τ_{imp} in Fig 2, the bunch becomes tight with increasing N_{B}.
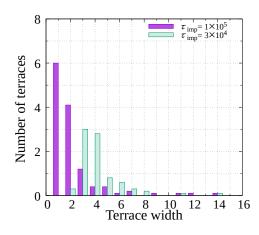
8

FIG. 4. (color online) Distributions of terrace widths that are smaller than 16 for $\tau_{\text{imp}} = 3 \times 10^4$ and $\tau_{\text{imp}} = 1 \times 10^5$. The data are averaged over 10 individual runs.

We regard steps as isolated when their upper side terrace and lower side terrace are longer than a critical width l_c. Because the number of terraces for which the width is wider than six is small in Fig. 4, we set l_c to six hereinafter. When we use this criterion, the average
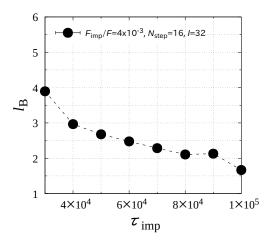

FIG. 5. Dependence of l_B on τ_{imp}. The data are averaged over 10 individual runs.

step distance in bunches l_B decreases with increasing τ_{imp} (Fig. 5).

Figure 6 shows the time dependence of N_{iso}. With increasing time, N_{iso} decreases and is just one or two in the systems in the last stage. Figure 7 shows how the average number of bunches in systems N_{BS} depends on time. As single steps gather and small bunches forms, N_{BS} increases with time in the initial stages. However, N_{BS} decreases with time in the later stages because N_B increases from the collision of bunches and N_{BS} seems to saturate in the
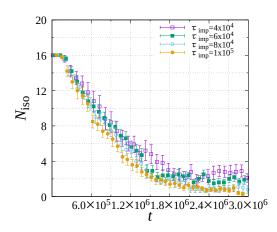
FIG. 6. (color online) Time dependence of N_B. The data are averaged over 10 individual runs.
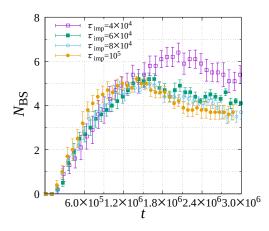

FIG. 7. (color online) Time dependence of N_{BS}. The data are averaged over 10 individual runs.

last stage.

In Fig. 8, we show the dependence of N_B in the last stage on τ_{imp}. Although the change in N_B is small in our simulation range of τ_{imp} because of the limited system size, N_B increases with increasing τ_{imp}.

The adatom density on surface σ_{imp} and the ratio of impurities incorporated into solid to solidified atoms ρ_{imp} in the last stage depend on τ_{imp}; see Figs. 9 and 10. Both σ_{imp} and ρ_{imp} increase with increasing τ_{imp}. In our previous paper [14], we supposed the impurity density c_{imp} obeys

$$\frac{dc_{imp}}{dt} = F_{imp} - \frac{c_{imp}}{\tau_{imp}}. \tag{5}$$

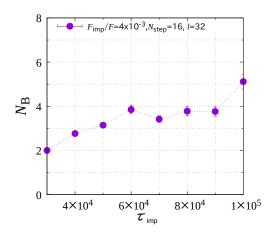We assumed that bunches with size N_B are formed equidistantly and that the separation

10

FIG. 8. (color online) Dependence of N_B in the last stage. The data are averaged over 10 individual runs.

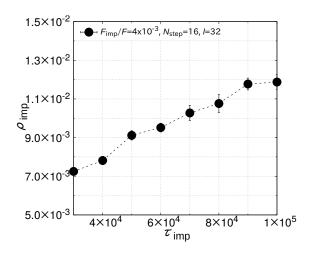

FIG. 9. Dependence of ρ_{imp} on τ_{imp} in the last stage. The data are averaged over 10 individual runs.

of steps from bunches does not occur. The incorporation of impurities in the solid phase occurs by advancing the lowest steps in bunches. When the distance between bunches is longer than the surface diffusion length, ρ_{imp} is given by

$$\rho_{imp} = \frac{\Omega \tau_{imp} F_{imp}}{N_B} \left[1 - \exp \left(-\frac{N_B^2 l}{\Omega x_s (F - F_{eq}) \tau_{imp}} \right) \right], \tag{6}$$

where Ω is the atomic area, l the step distance in a vicinal face, x_s the surface diffusion length defined as $x_s = \sqrt{D_s \tau}$, τ the lifetime of adatoms, and F_{eq} is given by c_{eq}/τ. In our simulations, $\tau = 512$ and $D_s = 1$, so that x_s is estimated to be 22.6. The prefactor in front of the parenthesis mainly changes ρ_{imp} because the exponential term on the right-hand side
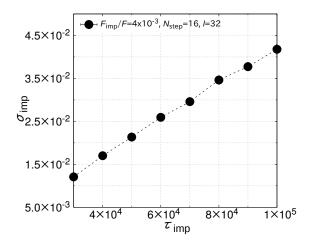
11

FIG. 10. Dependence of σ_{imp} on τ_{imp} in the last stage. The data are averaged over 10 individual runs.

of Eq. (6) is negligibly small. As the change in N_{B} is small in our simulation, the change in ρ_{imp} mainly is caused by τ_{imp}.

B. Dependence of step bunching on the coefficients of surface diffusion

Next, we changed D_{imp}/D and studied how surface diffusion of impurities affects the step bunching induced by impurities. We set the diffusion of adatoms to be much faster than that of impurities and performed simulations. Figure 11 shows snapshots of the step bunches formed by impurities. The ratio $D_{\mathrm{imp}}/D_{\mathrm{s}}$ is changed from 10^{-5} to 6×10^{-5}. N_{B} seems to decrease with increasing $D_{\mathrm{imp}}/D_{\mathrm{s}}$. From the snapshots, step bunching without the surface diffusion of impurities is not much different from that with the surface diffusion of impurities. However, the difference in the process of step bunching between these two cases is obvious from the time evolution of average step positions (Fig. 12).

Figures 12(a)–(f) show the time evolution of the average step positions for the samples in obtaining Figs. 11(a)–(f), respectively. Small bunches are formed in an early stage in Figs. 12(a) and (b). The bunches gather and large bunches separated by large terraces are formed in the last stage. The process of forming large bunches seems to be almost the same as that observed in Fig. 3. However, the separation and collision of single steps occur in a later stage in Figs. 12(c)–(f). In particular, large bunches are not formed in Figs. 12 (e) and (f). The separation and collision between small bunches and single steps are frequently
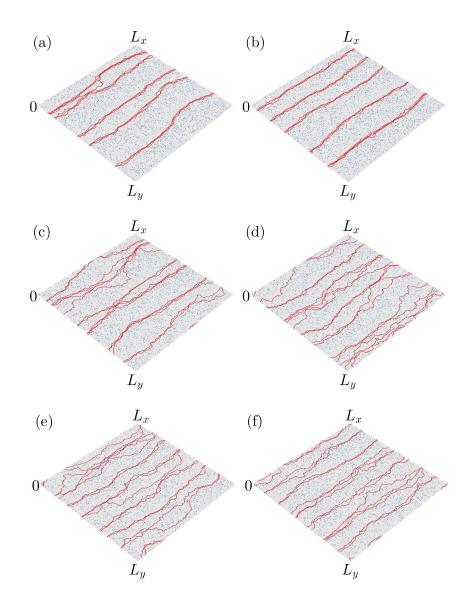
12

FIG. 11. (color online) Snapshots of a vicinal face in late stages during step bunching induced by impurities with the surface diffusion of impurities, where (a) $D_{\mathrm{imp}}/D_{\mathrm{s}} = 10^{-5}$ at $t = 3.5 \times 10^6$, (b) $D_{\mathrm{imp}}/D_{\mathrm{s}} = 2 \times 10^{-5}$ at $t = 3.5 \times 10^6$, (c) $D_{\mathrm{imp}}/D_{\mathrm{s}} = 3 \times 10^{-5}$ at $t = 3.5 \times 10^6$, (d) $D_{\mathrm{imp}}/D_{\mathrm{s}} = 4 \times 10^{-5}$ at $t = 3.6 \times 10^6$, (e) $D_{\mathrm{imp}}/D_{\mathrm{s}} = 5 \times 10^{-5}$ at $t = 3.5 \times 10^6$, and (f) $D_{\mathrm{imp}}/D_{\mathrm{s}} = 6 \times 10^{-5}$ at $t = 3.6 \times 10^6$. The blue dots on the surface represent impurities.

repeated. They affect the distribution of terrace widths. Because of the separation and collision of steps, not only the average terrace width becomes large but also the distribution of terrace widths becomes broad (Fig. 13).

Figure 14 shows the dependence of l_{B} on $D_{\mathrm{imp}}/D_{\mathrm{s}}$, where l_c is the same as that used in Fig. 6. l_{B} increases with increasing $D_{\mathrm{imp}}/D_{\mathrm{s}}$ and seems to saturate in a large $D_{\mathrm{imp}}/D_{\mathrm{s}}$
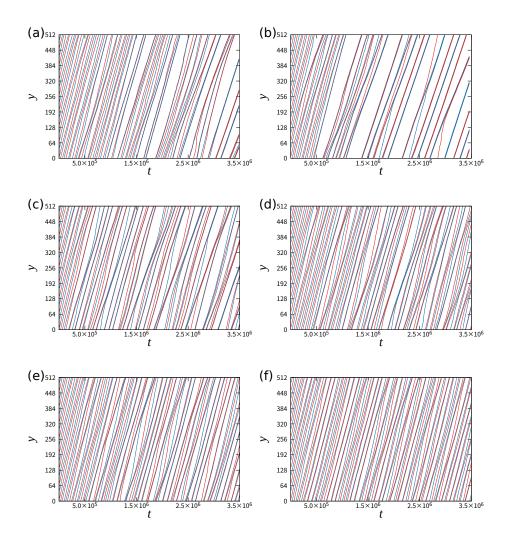
13

FIG. 12. (color online) Time evolution of step positions averaged in the x-direction for the samples used in Fig. 11(a)–(f). τ_{imp} is set to 10^5. $D_{\text{imp}}/D_{\text{s}}$ is (a) 1×10^{-5}, (b) 2×10^{-5}, (c) 3×10^{-5}, (d) 4×10^{-5}, (e) 5×10^{-5}, and (f) 6×10^{-5}.

region, where the separation and collision of steps frequently occur. The saturated value of l_{B} is larger than the maximum value of l_{B} in Fig. 5.

We analyze the properties of step bunches in more details. Figure 15 shows the time dependence of N_{iso} for some $D_{\text{imp}}/D_{\text{s}}$. N_{iso} decreases with increasing time due to the formation of step bunches but in the last stage increases with increasing $D_{\text{imp}}/D_{\text{s}}$. Almost all the steps are single steps when $D_{\text{imp}}/D_{\text{s}} = 8 \times 10^{-5}$. The time evolution of N_{BS} is opposite to that of N_{iso} (Fig. 16): N_{BS} increases with increasing time and the saturated value in the last stage decreases with increasing $D_{\text{imp}}/D_{\text{s}}$ (Fig. 17), in which the final value of N_{B} is not more than three. From Figs. 15–17, we find that a few small bunches form and step separation
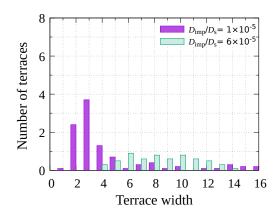
14

FIG. 13. (color online) Distributions of terrace widths that are smaller than 16 for $D_{\mathrm{imp}}/D_{\mathrm{s}} = 1 \times 10^{-5}$ and $D_{\mathrm{imp}}/D_{\mathrm{s}} = 6 \times 10^{-5}$. The data are averaged over 10 individual runs.
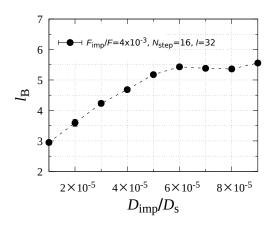

FIG. 14. Dependence of l_{B} on $D_{\mathrm{imp}}/D_{\mathrm{s}}$. The data are averaged over 10 individual runs.

frequently occurs when $D_{\mathrm{imp}}/D_{\mathrm{s}}$ is large.

We show how σ_{imp}, ρ_{imp}, and the growth rate of a vicinal face, R, depend on $D_{\mathrm{imp}}/D_{\mathrm{s}}$ in Figs. 18, 19, and 20, respectively. From Figs. 12(a) and (b), we find that the separation and collision of single steps hardly occur when $D_{\mathrm{imp}}/D_{\mathrm{s}} = 1 \times 10^{-5}$ and 2×10^{-5}. The surface diffusion of impurities is slow in these cases, so that the impurities in front of the step bunches prevent the lowest steps in the step bunches from advancing faster than the other steps in the bunches. Therefore the separation of steps from bunches does not occur, and ρ_{imp} is large because almost all the impurities in front of the step bunches are incorporated into the solid when the step bunches advance. When $D_{\mathrm{imp}}/D_{\mathrm{s}}$ is large, the impurities in front
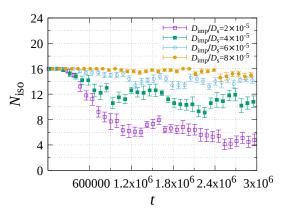
15

FIG. 15. (color online) Time dependence of N_{iso} on $D_{\text{imp}}/D_{\text{s}}$. The data are averaged over 10 individual runs.
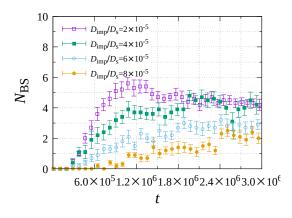

FIG. 16. (color online) Time dependence of N_{BS}. The data are averaged over 10 individual runs.

of the step bunches move away though surface diffusion before being incorporated into the solid. The effect that the impurities prevent the lowest steps from advancing is weakened. The impurities in front of the step bunches also move in the step bunches. These impurities prevent the steps in bunches from catching up to the lowest steps. Hence, separation of steps from step bunches becomes possible. When this separation, R increases as separated steps move faster than step bunches, and σ_{imp} decreases because the impurities swept by the separated steps increases. However, when $D_{\text{imp}}/D_{\text{s}}$ increases further, so many impurities move away before being incorporated into solid at single steps. Therefore, σ_{imp} increases again and ρ_{imp} decreases.
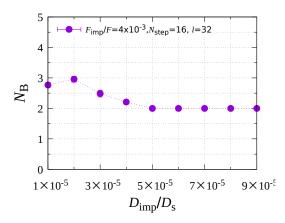
FIG. 17. (color online) Dependence of N_{B} in the last stage on $D_{\mathrm{imp}}/D_{\mathrm{s}}$. The data are averaged over 10 individual runs.
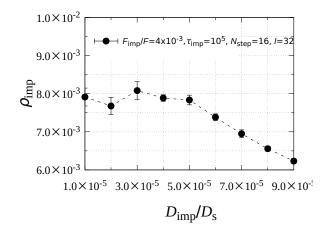

FIG. 18. Dependence of ρ_{imp} in the last stage on $D_{\mathrm{imp}}/D_{\mathrm{s}}$. The data are averaged over 10 individual runs.

IV. SUMMARY

We performed Monte Carlo simulations and studied the effects of both the evaporation and diffusion of impurities on step bunching induced by impurities. When we take into account the evaporation of impurities and neglect the surface diffusion of impurities, the step bunching proceeds by the collision of small bunches. When the evaporation of impurities increases, the effect of impurities on forming bunches is weakened and the size of bunches decreases, but the separation of steps from bunches does not occur in this instance.

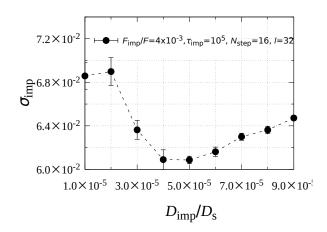The surface diffusion of impurities also weakens the effect of impurities on the formation

FIG. 19. Dependence of σ_{imp} in the last stage on $D_{\text{imp}}/D_{\text{s}}$. The data are averaged over 10 individual runs.
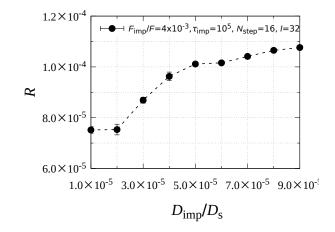

FIG. 20. Dependence of R on $D_{\text{imp}}/D_{\text{s}}$. The data are averaged over 10 individual runs.

of large bunches, and the separation of single steps occurs. The front of a bunch is the dirtiest area with impurities because the area is exposed to the vapor phase for the longest time. If the lowest step in a bunch tries to escape from the step bunches in the system without surface diffusion of impurities, the second lowest step in the bunch easily catches up with the lowest step because there are few impurities in front of the second lowest step. However, impurities can move even in the step bunch when the surface diffusion of impurities occurs. The impurities coming in front of the second lowest step probably prevent the second lowest step from catching up with the lowest step. Therefore, the lowest step can separate from the step bunch if the surface diffusion of impurities is sufficiently fast. We do not

18

have simulation results showing evidence for the above scenario directly. However, when we take into account Figs. 18–20, we believe the scenario we mentioned above is reasonable in explaining why the separation of steps occurs in the system with the surface diffusion of impurities.

ACKNOWLEDGMENTS

---

[1] N. Cabrera and D. A. Vermilyea, *Growth and Perpection of Crystals,*, Proceedings of the International Conference, Cooperstown, NY, Wiley, 393 (1958)

[2] W. K. Burton, N. Cabrera, and F. C. Frank, Philos. Trans. R. Soc. London, Ser. A **243**, 299 (1951).

[3] J. P. v. d. Eerden and H. Müller-Krumbhaar, Phys. Rev. Lett. **57**, 2431 (1986).

[4] D. Kandel and J. D. Weeks, Phys. Rev. Lett. **69**, 3758 (1992).

[5] D. Kandel and J. D. Weeks, Phys. Rev. B **49**, 5554 (1994).

[6] J. Krug, Euro. Phys. Lett. **60**, 788 (2002).

[7] J. Vollmer, J. Hegedüs, F. Grosse, and J. Krug, New J. Phys. **10**, 053017 (2008).

[8] M. Ranganathan and J. D. Weeks, Phys. Rev. Lett. **110**, 055503 (2013).

[9] M. Ranganathan and J. D. Weeks, J. Cryst. Growth, **393**, 35 (2014).

[10] J. F. Lutsuko, N. Gonzáles-Segredo, M. A. Durán-Olivencia, A. E. S. Van Driessche, and M. Sleutel, Cryst. Growth Des. **14**, 6129 (2014).

[11] J. F. Lutsko, A. E. S. Van Driessche, and M. A. Durán-Olivencia, D. Maes, and M. Sleutel, Phys. Rev. Lett. **116**, 015501 (2016).

[12] M. Sleutel, J. Lutsko, and A. E. S. Van Driessche, Cryst. Growth Des. **18**, 171 (2018).

[13] M. Sato, J. Phys. Soc. Jpn. **86**, 114603 (2017)

[14] M. Sato, Phys. Rev. E **97**, 062801 (2018) .

[15] M. Sato and M. Uwaha, Phys. Rev B **51** 11172 (1995).

[16] M. Sato and M. Uwaha, Surf. Sci. **442** 318 (1999).

[17] M. Sato and M. Uwaha, Surf. Sci. **493** 494 (2001).

[18] M. Vladimirova, A. De Vita, and A. Pimpinelli, Phys. Rev. B **64**, 245420 (2001).

[19] G. Ehrlich and F. G. Hudda, J. Chem. Phys. **4**, 1039 (1966).

[20] R. L. Schwoebel, J. Appl. Phys. **40**, 614 (1969).

[21] M. Uwaha and Y. Saito, Phys. Rev. Lett. **68**, 224 (1992).

[22] M. Uwaha and Y. Saito, Surf. Sci. **283**, 366 (1993).

[23] Y. Saito, T. Sakiyama, and M. Uwaha, J. Cryst. Growth . **128**, 82 (1993).

[24] Y. Saito and M. Uwaha, Phys. Rev. B **49**, 10677 (1994) .

[25] M. Sato, M. Uwaha and Y. Saito, Phys. Rev. B **62** 8452 (2000).